SAKARYA ÜNİVERSİTESİ
FEN BİLİMLERİ ENSTİTÜSÜ DERGİSİ

Sakarya University Journal of Science
SAUJS

ISSN 1301-4048 e-ISSN 2147-835X Period Bimonthly Founded 1997 Publisher Sakarya University
http://www.saujs.sakarya.edu.tr/

Title: Comparative Evaluation of Alginate-Gelatin Hydrogel, Cryogel, and Aerogel Beads as a Tissue Scaffold

Authors: Ece BAYIR

Recieved: 2022-04-05 00:00:00

Accepted: 2023-01-28 00:00:00

Article Type: Research Article

Volume: 27
Issue: 2
Month: April
Year: 2023
Pages: 335-348

How to cite
Ece BAYIR; (2023), Comparative Evaluation of Alginate-Gelatin Hydrogel, Cryogel, and Aerogel Beads as a Tissue Scaffold. Sakarya University Journal of Science, 27(2), 335-348, DOI: 10.16984/saufenbilder.1098637
Access link
https://dergipark.org.tr/en/pub/saufenbilder/issue/76551/1098637

Sakarya University Journal of Science 27(2), 335-348, 2023

Comparative Evaluation of Alginate-Gelatin Hydrogel, Cryogel, and Aerogel Beads as a Tissue Scaffold

Ece BAYIR*[1]

Abstract

Hydrogels are frequently used in tissue engineering and regenerative medicine, drug delivery, and environmental remediation. Alginate and gelatin, which are frequently used natural polymers to form hydrogels, were chosen in this study to form a core-shell structured hydrogel. Cryogels and aerogels were obtained by drying hydrogels with different methods, freeze-drying, and the continuous flow of supercritical CO_2, respectively. The potential use of hydrogels, aerogels, and cryogels as a tissue scaffold was evaluated comparatively. Characterizations of materials were determined morphologically by scanning electron microscope and computed-micro tomography, chemically by energy dispersive spectroscopy, and mechanically by the dynamic mechanical analyzer. In addition, the cytotoxic effect of all structures was analyzed by the WST-1 method and the localization of the cells in these structures was determined by microscopic methods. All scaffolds show non-cytotoxic effects. Cryogels have the highest porosity (85.21 %) and mean pore size values (62.3±26.8 μm). Additionally, cryogels show high water retention capacity (782±53.5%) than aerogels (389±2.5%) for 24 h. The elastic modulus values were <10 kPa, which is suitable for brain, bone marrow, spleen, pancreas, fat, kidney, and skin tissue engineering, for all types of beads. It has been determined that cryogel and hydrogel beads are more suitable for cell adhesion and migration in this study.

Keywords: Tissue engineering, scaffold, sodium alginate, gelatin

1. INTRODUCTION

Hydrogels are materials that are composed of hydrophilic polymers, are insoluble in water, and have a high water-holding capacity in their structures. Physical and/or chemical crosslinking methods are used to form hydrogels from polymers [1]. Weak interactions occur between polymer networks during physical gelation, and strong chemical bonds are formed between polymer chains during chemical gelation [2]. For this reason, polymers formed by physical methods are easily degraded, while polymers obtained by chemical methods are not. Hydrogels can be classified as synthetic, semi-synthetic, and natural. Synthetic hydrogels are generally synthesized by

* Corresponding author: ece.bayir@ege.edu.tr
[1] Ege University Central Research Test and Analysis Laboratory Application and Research Center (EGE-MATAL), Ege University, 35100, Izmir, Turkey
E-mail: ece.bayir@ege.edu.tr
ORCID: https://orcid.org/0000-0003-4886-3860

polymerization of vinyl monomers, and natural hydrogels are obtained from natural polymers such as polynucleotides, polypeptides, and polysaccharides [3]. In recent years, studies have been carried out on the use of hydrogels in many different areas such as drug delivery systems, drug encapsulation, tissue engineering, and environmental remediation [4-8]. The most used polymers to obtain hydrogels are natural polymers due to their high biocompatibility.

Sodium alginate, natural water-soluble salt of alginic acid, is an anionic polysaccharide composed of (1-4) linked β-D-mannuronic acid (M) and α-L-guluronic acid (G) obtained from the cell wall of brown algae [9]. It is a highly biocompatible, biodegradable, and relatively cheap biopolymer. The ability to form hydrogels is one of the main properties of alginate. This property of sodium alginate is mainly due to the replacement of Na^+ in the guluronic acid residues with different divalent cations (Ca^{2+}, Sr^{2+}, Ba^{2}+, etc.) [10].

Gelatin is a cheap, easily obtainable biopolymer with high biocompatibility, which is the denatured collagen of animals such as porcine, bovine, and fish. It is non-immunogenic, biodegradable, and easily soluble in water at 37°C [11]. Because of that its mechanical and chemical properties can be modified easily, cells can adhere easily to gelatin, and it promotes cell proliferation; it can be used as a tissue engineering scaffold and drug delivery agent for biomedical applications [12]. There are many studies performed with alginate-gelatin based 3D tissue scaffolds. In the most of these studies, tissue scaffolds are obtained by 3D printer. Chawla et al. used alginate-gelatin based hydrogel and MG63 osteoblast cells as bioink, and thus the entire hydrogel and cell mixture was bioprinted [13]. In the study of Pan et al., after the alginate-gelatin based scaffold was 3D-printed, it was lyophilized, and mouse bone mesenchymal stem cells were seeded in both hydrogel and cryogel form of the scaffolds, and the effects of the physical and physicochemical properties of the scaffolds on tissue regeneration were investigated [14]. Baldino et al., different from the other researchers, obtained aerogels by mixing alginate and gelatin in a container, and after supercritical gel drying, their usability for tissue engineering was evaluated [15].

Hydrogels can be dried by various methods to obtain structures with different properties. The pores usually collapse when the solvent evaporates in the hydrogel, which is dried under atmospheric conditions (xerogel). Hydrogels dried with the freeze-drying method and drying with a continuous flow of supercritical CO_2 are called cryogel and aerogel, respectively [16]. The pore structures of hydrogels dried by these two methods are preserved, and therefore their use for biomedical and environmental purposes is more common.

In recent researches, alginate-gelatin based hydrogels, cryogels, and aerogels have been studied by obtaining various methods; however, the use of these structures produced by the same technique as tissue scaffolds has not been examined comparatively. This study aims to compare the physical, chemical, biological, and mechanical properties of alginate-gelatin hydrogel, cryogel, and aerogel beads and to evaluate their suitability for tissue engineering scaffold.

2. MATERIALS AND METHODS

2.1. Alginate-Gelatin Hydrogel, Cryogel and Aerogel Bead Synthesis

Alginic acid sodium salt (71238, Sigma-Aldrich, USA), type A gelatin (G2500, Sigma-Aldrich, USA), and $CaCl_2$ (223506, Sigma-Aldrich, USA) powders were used for the synthesis of alginate-gelatin hydrogel beads. Alginic acid sodium salt was stirred in the ultra-pure water (UPW) at 1.25% (w/v) concentration until dissolving and pH

was adjusted to 7.4 with NaOH (S5881, Sigma-Aldrich, USA). Gelatin (%10 (w/v)) was dissolved in UPW in another bottle at 50°C for overnight, and $CaCl_2$ (1.5% (w/v)) was added and stirred for 1 h. Since sodium alginate cross-linked by divalent cations, $CaCl_2$ was added into gelatin solution for internal Ca^{+2} source for alginate coating.

Alginate solution was poured into the beaker and stirred with a magnetic stirrer. The syringe was filled with gelatin solution and dripped into the alginate solution (Figure 1). This production procedure was adapted from Baruch and Machluf's work [17]. Alginate-gelatin beads were rinsed with UPW three times. To produce cryogel and aerogel, hydrogel beads were dried with two different methods (freeze-drying and critical point drying).

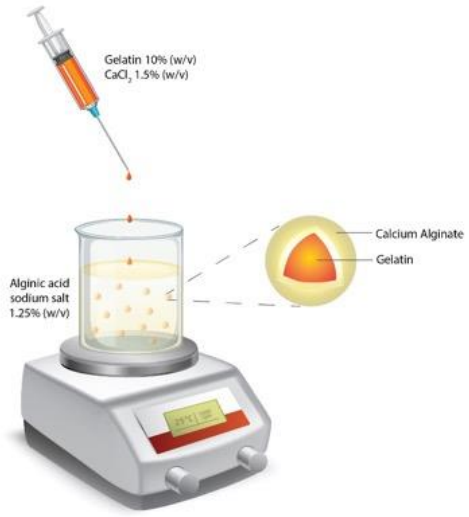

Figure 1 Alginate-gelatin bead production scheme.

Beads were frozen at -20°C before the freeze-drying process and kept in the freeze-dryer (1.2 D Alpha Plus, Martin Christ, Germany) for 24 h. For supercritical CO_2 drying method, hydrogel beads were placed into the sample holder of the critical point drier (CPD, Leica EM CPD300, Germany) in absolute ethanol for 2 h.

2.2. Characterization of Beads

2.2.1. Morphological Observation and Elemental Analysis

Cryogels and aerogels were analyzed with the scanning electron microscopy (SEM) technique for evaluating their morphology. Before the observation, the beads were cross-sectioned and, both beads and sectioned parts were sputter-coated with 7 nm Au-Pd. The observations were performed by Thermo Scientific Apreo S, at 5 kV accelerating voltage. Energy dispersive X-rays detector (EDS) of SEM was used to perform elemental analysis of the samples. Both core and shell structures were analyzed.

2.2.2. Mechanical Analysis

Compressing test was operated on a dynamic mechanical analyzer (DMA, Q800, TA Instruments) to determine the mechanical properties of hydrogels, cryogels, and aerogels. Samples were placed between compression clamps. Tests were performed at 0.5 N/min ramp force to 18 N and 37°C. Hydrogels were analyzed with DMA in wet form, while cryogels and aerogels were analyzed in dry form.

2.2.3. Porosity and Thickness Distribution

The average pore size, porosity, and thickness distribution of the beads were analyzed with Micro Computed Tomography (Micro-CT) device (µCT50, Scanco Medical, Switzerland). Samples were scanned at 70 kVp energy, 114 µA intensity, 20 µm voxel size, and 300 ms integration time. After the scanning process, the samples were analyzed with an evaluation program (Scanco Medical, Switzerland). Porosity was calculated according to the following formulae.

$$Porosity\ (\%) = \frac{Total\ volume - Solid\ volume}{Total\ volume} \times 100$$

2.2.4. Hydration Degree

Cryogel and aerogel beads were weighed separately with three replicates. All beads were weighed after keeping in UPW for 3 h and 24 h at 37°C. Hydration degree was calculated with formulae below.

$$Hydration\ degree\ (\%) = \frac{Wet\ weight - Dry\ weight}{Wet\ weight} \times 100$$

2.3. Biological Analysis

2.3.1. Cell Culture

In order to examine the use of produced alginate-gelatin hydrogels, cryogels, and aerogels as tissue scaffolds, in vitro cytotoxicity tests were performed on the scaffolds within the scope of BS EN ISO 10993-5-2009 standard [18], and cell images were taken under an inverted fluorescence microscope (Zeiss Axio Vert A1, Germany) to determine the localization of the cells seeded in the scaffolds. L929 mouse fibroblast cell line (CCL-1, ATCC, USA), recommended in the standard, was used for the cytotoxicity test.

Cells were cultivated in Minimum Essential Medium Alpha Modification (MEMA-RXA, Capricorn Scientific, Germany) supplemented with 10% (v/v) fetal bovine serum (FBS, 10500-064, Gibco, Germany), 2 mM L-Glutamine (25030-024, Gibco, Germany), 1 mM sodium pyruvate (S8636, Sigma Aldrich, Germany), and 10 µg/mL gentamicin (GEN-10B, Capricorn Scientific, Germany). Cells were incubated in 5% CO_2 and 95–98% humidified atmosphere at 37°C. Cells were trypsinized (25200-056, Gibco, Germany) and passaged until reaching desired cell number.

2.3.2. Cytotoxicity

The cytotoxicity of scaffolds on L929 cells was analyzed with the WST-1 assay (05015944001, Cell Proliferation Reagent WST-1, Merck, Germany). For this purpose, a calibration chart was drawn first to optimize the incubation time of cells with WST-1 and to find the absorbance values corresponding to certain cell numbers. Cells were trypsinized and counted with a Neubauer Hemocytometer and seeded into a 96-well plate at certain concentrations between 1×10^3 - 1×10^5 cells/well and incubated for 4 h. At the end of the incubation time, 10 µL of WST-1 was added to the wells and analyzed in a 450 nm/630 nm microplate reader at different times in the range of 0.5 - 4 h.

To perform the cytotoxicity test, scaffolds were sterilized overnight in 70% (v/v) Ethanol. After the scaffolds were rinsed 3 times with PBS, scaffolds were extracted in culture medium at a concentration of 0.2 g/mL for 24 h at 37°C. Extraction ratio (0.2 g/mL) was selected according to the "Standard surface areas and extract liquid volumes" table in *ISO 10993-12:2009 Biological evaluation of medical devices, Sample preparation and reference materials*. L929 cells were seeded at 1×10^4 cells/well in a 96-well plate and incubated for 24 h. At the end of the incubation period, the medium on the cells was removed and the extracted medium was added in a volume of 100 µL (n=3). After the cells were incubated for 24 h, 10 µL of WST-1 was added to the cells and analyzed after 60 min in a 450/630 nm microplate reader (ELx800, BioTek, USA).

2.3.3. Monitoring Cell Localization in the Scaffolds

Cells were counted and seeded in the scaffolds at 1×10^6 cells/scaffold after the scaffolds were conditioned in a culture medium for 24 h. Cells were seeded with a 1 mL syringe in a volume of 100 µL. After 24 h incubation time, cell nuclei were stained with 4',6-Diamidino-2-phenylindole dihydrochloride (DAPI, D9542, Sigma-Aldrich, Germany). DAPI (0.1 µg/mL) was diluted in PBS, and all scaffolds were

incubated in DAPI solution in the dark after the rinsing with PBS. The cells were monitored under an inverted fluorescent microscope [19].

2.3.4. Statistical analysis

All quantitative experiments were performed in at least three replicates (n=3). For statistical analysis, the Shapiro Wilk test was used to determine whether the data fit the normal distribution, and One-Way Analysis of Variance (ANOVA) was applied (95% confidence interval) for the data sets that fit the normal distribution. Tukey was chosen as the post-hoc method to determine the different groups.

2. RESULTS AND DISCUSSION

3.1. Characterization of Beads

3.1.1. Morphological Observation and Elemental Analysis

All three types of scaffolds are in the form of ellipses, and the average dimensions of hydrogels are 5.014±0.123 × 5.621±0.085 mm (W×L), cryogels are 2.789±0.152 × 2.951±0.105 mm (W×L), and aerogels are 2.213±0.201 × 2.623±0.074 mm (W×L).

Both cryogel and aerogel beads were observed with SEM in order to analyze the morphological difference. Hydrogel beads were not observed with the SEM device because of contained water. It is clearly seen that the size of cryogel beads was larger, and the core structure of the cryogel beads has wider pores than aerogel beads (Figure 2).

Since the cryogels are frozen before the drying process, the volume of the hydrogel increases as the water freezes. Ice crystals between the pores of the hydrogel also expands the pores. For this reason, the morphological structures of cryogel and aerogel scaffolds are different from each other, and this result is in line with previous studies [20, 21].

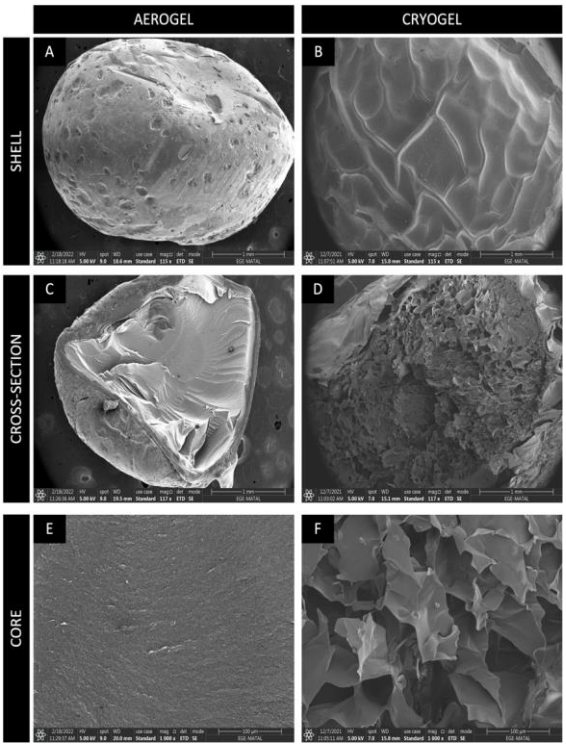

Figure 2 SEM images of aerogel and cryogel beads. A-B. Shell structure of aerogel and cryogel beads, respectively. Scale bars correspond to 1 mm. C-D. Cross-sections of aerogel and cryogel beads, respectively. Scale bars correspond to 1 mm. E-F. Core structure of aerogel and cryogel beads, respectively. Scale bars correspond to 100 μm.

When the cross-section of aerogel beads is observed in more detail, it can be seen the beads have morphologically three different layers (Figure 3). The elemental analysis of outer layer (shell) results shows that the outer wall of aerogels consists of C, H, O and Ca. Na^+ in alginic acid sodium salt solution was replaced by the Ca^{2+} in the gelatin-$CaCl_2$ solution in the core structure and formed calcium alginate ($CaC_{12}H_{14}O_{12}$). The EDS results of the core structure show that it consists of C, H, O, and N elements in the molecular formula of gelatin ($C_{102}H_{151}N_{31}O_{39}$). However, Ca^{2+} was also found in the intersection of core and shell structures.

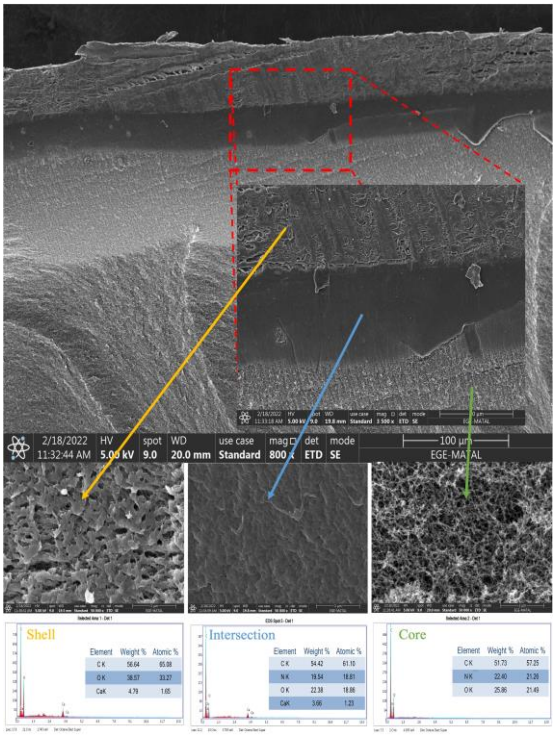

Figure 3 SEM images and EDS results of aerogel cross-section. The outer wall of the aerogel is calcium alginate, and the inner wall is gelatin structured. There is an intersection area, and this part contains both gelatin and calcium alginate properties.

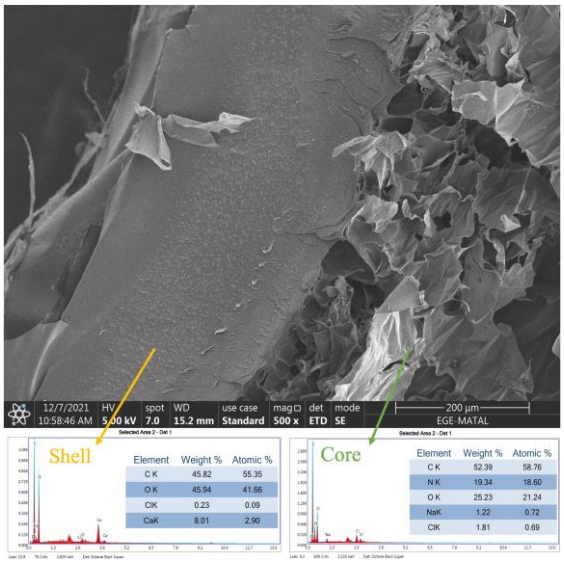

Figure 4 SEM images and EDS results of cryogel cross-section. Contrary to the aerogel, a sharp transition is observed between the core-shell structure in the cryogel. According to EDS results, the core structure consists of gelatin, and the shell structure consists of calcium alginate.

EDS results of cryogel show that the core consist of Na^+ and Ca^{2+} as well as the elements in the molecular formula of gelatin (Figure 4). It is thought that Na^+ originates from alginic acid sodium salt ($NaC_6H_7O_6$) and Cl^- originates from $CaCl_2$ salt. The shell structure consists of C, H, O, Cl and Ca, and it indicates that calcium alginate is formed similarly to aerogel beads.

3.1.2. Mechanical Analysis

The compression tests of scaffolds were performed on DMA device and the stress-strain graph obtained is given in Figure 5. The elastic moduli of the beads were calculated from the linear slope on the stress/strain curves. The elastic moduli of hydrogel, cryogel and aerogel were found 7.1 kPa, 4.2 kPa, and 3.8 kPa, respectively.

It is known that the elastic modulus of the scaffolds affects the behavior of cells [22]. Therefore, researchers try to choose a scaffold whose mechanical properties match those of the tissue being formed. Since the elastic modulus values of beads are <10 kPa, the tissue scaffolds produced are suitable for tissue engineering of brain, bone marrow, spleen, pancreas, fat, kidney and skin [23, 24].

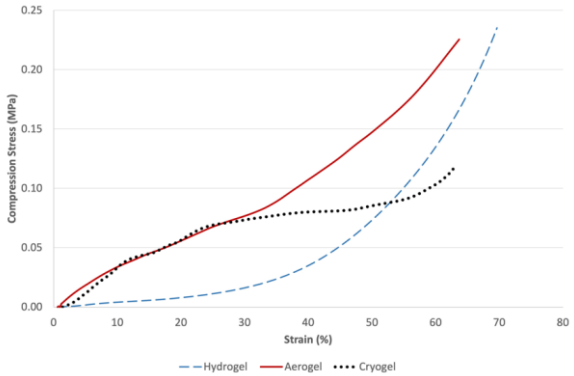

Figure 5 Compression Stress - Strain graph of hydrogel, aerogel, and cryogel.

Mechanical properties of hydrogels, cryogels, and aerogels can be changed by changing different parameters such as the concentration of divalent cations that play a role in the gelation of sodium alginate, the

concentration of crosslinking agents such as glutaraldehyde, treatment time, and production methods [10]. For this reason, it should not be considered that the tissue engineering materials produced are limited to their use only for the specified tissues because mechanical properties of beads can be easily changed for desired tissue.

3.1.3. Porosity and Thickness Distribution

The 2D images obtained after scanning the scaffolds in the Micro-CT device were transformed into 3D models with the Evaluation Program. Figures 6, 7 and 8 show hydrogel, cryogel and aerogel models, respectively. 3D models of beads are given in A and B, pore size distributions are given in C and D, and thickness distributions are given in E and F. The core-shell structure can be seen in these models. The pore sizes and the wall thickness of the scaffold are colored according to the size. The smallest pores are dark blue, and the largest pores are red in the color scale (C-D). Similarly, in the thickness distribution, the thinnest part appears in dark blue and the thickest part in red (E-F).

When the hydrogel and aerogel models are examined, a distinctive shell structure can be seen (Figure 6 and 8). In both models, the porosity of the shell structure is quite low compared to the core structure. The wall thicknesses are higher in the calcium alginate shell than in the gelatin core. For this reason, the use of these structures for drug delivery can also be considered. However, unlike the other two models, a distinct shell structure is not observed in the cryogel. In addition, there are larger diameter pores in the core structure compared to other models (Figure 7).

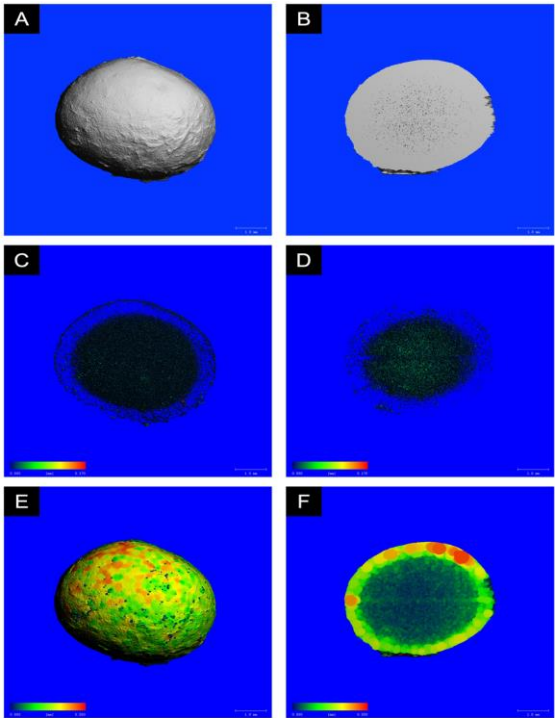

Figure 6 3D models of hydrogel beads. A. Overall 3D model, B. Cross-section of 3D model, C. Overall pore size distribution model, D. Cross-section of pore size distribution model, E. Overall thickness distribution model, F. Cross-section of thickness distribution model of the bead. Scale bars correspond to 1 mm.

The porosity results were determined as 5.18%, 57.46%, and 85.21% for hydrogel, aerogel, and cryogel, respectively. Hydrogel has a nanoporous structure as well as micro and macroporous structures. Nanopores are preserved while hydrogel is dried with supercritical CO_2 and the same structures observed in aerogels. Nanopores in the core structure of aerogels can be observed in SEM results. Since it is not possible to determine the nanopores with Micro-CT, porosity values were obtained as a result of the evaluation of only the micro and macropore structures as a result of the Micro-CT analysis. It is thought that the reason for obtaining low porosity of the hydrogel is that almost all pores in its structure are filled with water, and due to the inability of the Micro-CT device to distinguish well enough the radiopacity of gel structure and water.

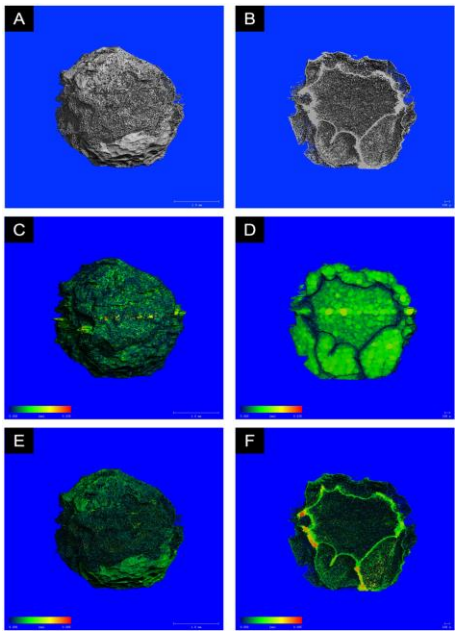

Figure 7 3D models of cryogel beads. A. Overall 3D model, B. Cross-section of 3D model, C. Overall pore size distribution model, D. Cross-section of pore size distribution model, E. Overall thickness distribution model, F. Cross-section of thickness distribution model of the bead. Scale bars correspond to 1 mm.

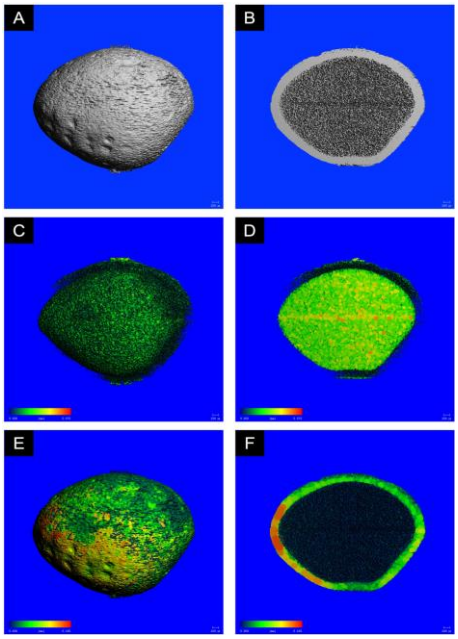

Figure 8 3D models of aerogel beads. A. Overall 3D model, B. Cross-section of 3D model, C. Overall pore size distribution model, D. Cross-section of pore size distribution model, E. Overall thickness distribution model, F. Cross-section of thickness distribution model of the bead. Scale bars correspond to 100 µm.

When the pore size distribution graphs are examined, it is seen that it is distributed in a wide pore size range in cryogel (Figure 9). The highest mean pore diameter (62.3±26.8 µm), and the lowest wall thickness (85 µm) were seen in the cryogel (Table 1). It is an expected result that the highest pore diameter is in the cryogel due to the expansion of water while freezing. In addition, these results obtained from Micro-CT support the SEM results.

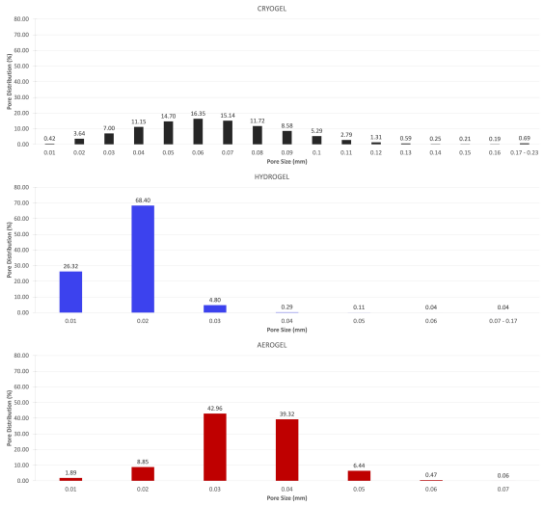

Figure 9 Pore size distribution of hydrogel, cryogel, and aerogel beads.

Table 1 Mean and maximum pore size and thickness values of hydrogel, cryogel, and aerogel.

	Pore Size (µm)		**Thickness (µm)**	
	Mean (±SD)	**Max**	**Mean (±SD)**	**Max**
Hydrogel	18±6.3	170	191.1 ±132.5	550
Cryogel	62.3 ±26.8	230	24.9±15 .1	85
Aerogel	31.5 ±7.9	70	59.6±4. 1	165

3.1.4. Hydration Degree

Hydration degree measurement was carried out in cryogels and aerogels in 3 hours and 24 hours. There was no statistical difference in the water holding capacity of aerogels for 3 and 24 hours, but a significant difference was observed in the water holding capacity of cryogels in 24 hours compared to 3 hours. In addition, in the results obtained in both

time zones, it was determined that the water holding capacity of cryogels was statistically higher than aerogels ($p<0.05$). While the aerogels held 334±19% water in 3 h, this value was determined as 389±2.5% in 24 h. On the other hand, the cryogels hold 563±55% in 3 h and 782±53.5% in 24 h (Figure 10). Since cryogels are characterized by their high water retention abilities, they are suitable candidates for use in soft tissue engineering and regenerative medicine, and the data obtained in this study also support these results [25].

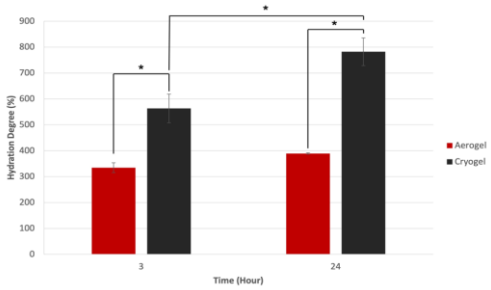

Figure 10 Hydration degree graph of aerogel and cryogel in 3 h and 24 h. The water holding capacity of cryogel is statistically higher than aerogel in both times. Also, the significant difference is observed in the water holding capacity of cryogels in 24 h compared to 3 h ($p<0.05$).

3.2. Biological Analysis

3.2.1. Cytotoxicity

It is necessary to determine the optimum incubation time to be applied on different cells to get the best results in the WST-1 cell proliferation test method. A calibration graph was obtained both to determine the optimum incubation time of WST-1 for L929 cells and to convert the absorbance data obtained as a result of the cytotoxicity test to the number of cells (Figure 11). After the cells were seeded in different concentrations between 1×10^3 - 1×10^5 cells/well, they were incubated for 4 h for their attachment and four different incubation times of 30 min, 1 h, 2 h and 4 h were tested for WST-1 analysis. The trendline R^2 value obtained was obtained in the highest on 1 h results (unpublished data). For this reason, a calibration chart for 1 h was used to determine the number of cells corresponding to absorbance.

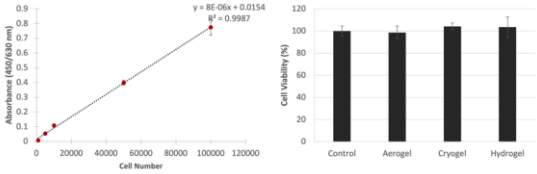

Figure 11 Calibration graph of WST-1 test on L929 cell line and cytotoxicity results of aerogel, cryogel, and hydrogel. There is no significant difference between all groups for cell viability ($p<0.05$).

The cytotoxic effects of aerogel, cryogel, and hydrogel beads on L929 cells were examined with the WST-1 analysis, and there was no statistically significant difference between viability of control and experimental groups at the end of the 24 h ($p<0.05$). According to the BS EN ISO 10993-5-2009 standard, the material has a cytotoxic effect when the cell viability is below 70% [18]. In this case, all potential scaffolds show non-cytotoxic effects. It has also been shown in previous studies that alginate and gelatin, which are natural polymers, do not have a cytotoxic effect [26, 27].

3.2.2. Monitoring cell localization in the scaffolds

In order to determine the localization of the cells in the scaffold, which were conditioned overnight in culture medium, after 24 h incubation time, the cells were monitored both under an inverted microscope and under a fluorescence microscope after staining with DAPI. It was observed that the cells were best distributed on the cryogel scaffold, and the number of cells was highest in these scaffolds. It was determined that the least number of cells and the worst distribution in the scaffold were in the aerogel. Although the number of cells in hydrogels is higher than in aerogel, the distribution of cells is not homogeneous as in cryogel (Figure 12-14).

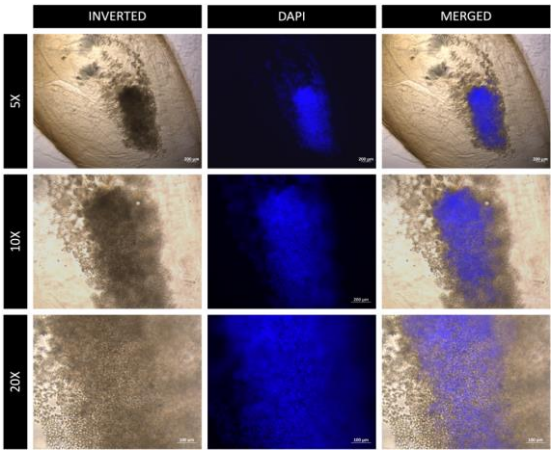

Figure 12 Cell localization in hydrogel tissue scaffolds. The first column shows inverted microscopy images of cells on 5X, 10X, and 20X magnifications, respectively. The second column shows DAPI stained cells on 5X, 10X, and 20X magnifications, respectively. The third column shows merged images of inverted microscopy images and fluorescent microscopy images on 5X, 10X, and 20X magnifications, respectively.

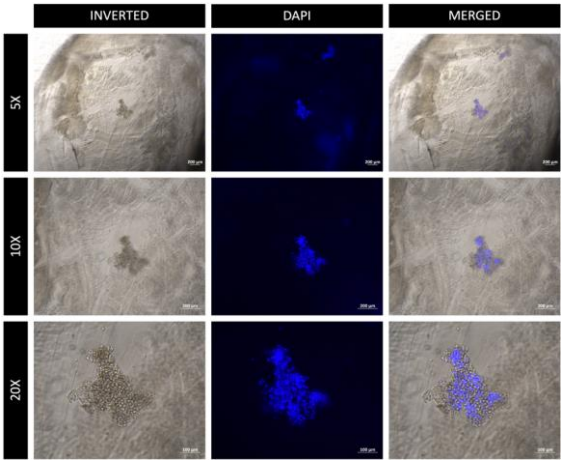

Figure 13 Cell localization in aerogel tissue scaffolds. The first column shows inverted microscopy images of cells on 5X, 10X, and 20X magnifications, respectively. The second column shows DAPI stained cells on 5X, 10X, and 20X magnifications, respectively. The third column shows merged images of inverted microscopy images and fluorescent microscopy images on 5X, 10X, and 20X magnifications, respectively.

It is thought that the reason for this situation is that the pore sizes in the cryogel are larger than the other scaffolds and cells can distribute more homogeneously. In this way, cells can migrate more easily within the scaffold, and thanks to the increased mass transfer due to the porous structure, they can reach the nutrient medium and oxygen more easily [28].

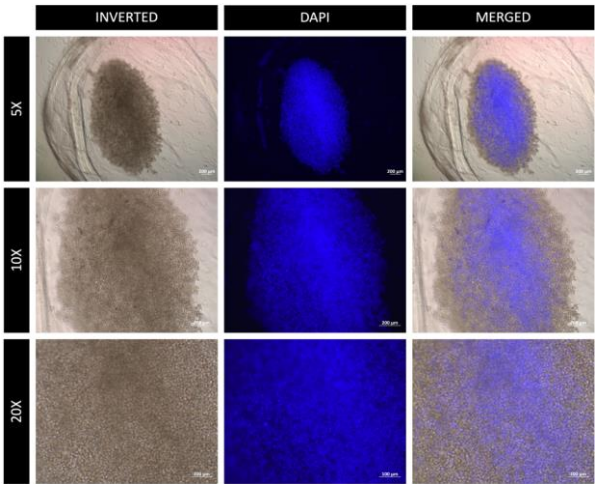

Figure 14. Cell localization in cryogel tissue scaffolds. The first column shows inverted microscopy images of cells on 5X, 10X, and 20X magnifications, respectively. The second column shows DAPI stained cells on 5X, 10X, and 20X magnifications, respectively. The third column shows merged images of inverted microscopy images and fluorescent microscopy images on 5X, 10X, and 20X magnifications, respectively.

Different methods can be used for cell seeding into the scaffold. It has been shown that the seeding of cells during the formation phase of hydrogels gives more successful results for cell distribution in the scaffold [29]. In addition, cell and scaffold materials can be mixed and used as bioink in bioprinters [13], in this method the cells are also distributed homogenously within the scaffold. Apart from these methods, cells can be directly seeded on the scaffold after the scaffold is formed. When this method is used, the porosity of the scaffold should be high, and the pore diameters should be suitable for cell migration. Thus, even if cells are seeded on the surface of the scaffold, they can migrate into the scaffold. In this study, a different cell seeding strategy was chosen from all these techniques. This is because if cells are mixed with hydrogel during scaffold fabrication, cells would die

during aerogel and cryogel formation. In order to do a comparative evaluation of hydrogel, cryogel, and aerogel scaffolds in terms of cell distribution, the same cell seeding procedure should be used for all scaffolds. For this reason, it was preferred to use post-production cell seeding methods instead of mixing the cells directly into the alginate-gelatin hydrogel. However, it was decided that direct cell seeding on the scaffold, which is a classical method, is not a correct strategy within the scope of this study. Because, especially in aerogels and hydrogels, the pore diameters of the shell are considerably lower than the core of the scaffolds. Since cells were not thought to migrate to the core of the scaffold when they were seeded on the scaffold surface, the cells were seeded by injecting them directly into the core with a syringe.

As a result of this study, it was decided that cryogel is the most suitable structure to be used as tissue scaffold among these three forms since it has higher pore diameters, higher porosities, and therefore the cell distribution within the scaffold is more homogeneous compared to other scaffold types. Although it seems more appropriate to use cryogels as tissue scaffolds in terms of cell distribution and adhesion, the use of hydrogels is also quite suitable. As mentioned above, more successful results can be obtained when cells are seeded during hydrogel formation. Aerogels, on the other hand, do not seem appropriate for 3D tissue culture inside of the bead due to the nano-sized pores in their structure, low hydration degree, and low cell adhesion. However, by attaching cells to the surface of aerogels, these scaffolds can be used as micro/macro carriers in bioreactors.

4. CONCLUSION

In this study, cryogels and aerogels were obtained by drying alginate-gelatin hydrogel beads with different methods (freeze-drying and critical point drying). The physical, chemical, biological, and mechanical properties of hydrogels, cryogels, and aerogels for their use as a tissue scaffold were comparatively investigated. According to the results obtained, all potential scaffolds are non-cytotoxic and their mechanical properties are suitable for soft tissue engineering. It was seen that cryogels with the highest pore diameter gave the most suitable results for cell adhesion and distribution. However, it is known that different cell seeding methods also give successful results for hydrogels. On the other hand, aerogel beads are not satisfactory for cultivating cells inside the bead due to their nanoporous structure. It can be used as a micro/macro carrier in bioreactors by cell adhesion to the surface of these structures or as a drug delivery agent because of the thick shell structure.

Acknowledgments
I thank Ege-MATAL and Prof. Dr. Suna Timur for laboratory facilities, and Dr. Raif İlktaç for his help.

Funding
The author has not received any financial support for the research, authorship, or publication of this study.

The Declaration of Conflict of Interest/ Common Interest
No conflict of interest or common interest has been declared by the authors.

Author's Contribution
E.B: Conceptualization, literature review, formal analysis, data collection, designing and drawing the figures, writing, reviewing, and editing.

The Declaration of Ethics Committee Approval
This study does not require ethics committee permission or any special permission.

The Declaration of Research and Publication Ethics
The author of the paper declare that I comply with the scientific, ethical and quotation

rules of SAUJS in all processes of the paper and that I do not make any falsification on the data collected. In addition, I declare that Sakarya University Journal of Science and its editorial board have no responsibility for any ethical violations that may be encountered, and that this study has not been evaluated in any academic publication environment other than Sakarya University Journal of Science.

REFERENCES

[1] R. Parhi, "Cross-Linked Hydrogel for Pharmaceutical Applications: A Review," Advanced pharmaceutical bulletin, vol. 7, no. 4, pp. 515-530, 2017.

[2] M. F. Akhtar, M. Hanif, N. M. Ranjha, "Methods of synthesis of hydrogels … A review," Saudi Pharmaceutical Journal, vol. 24, no. 5, pp. 554-559, 2016.

[3] I. M. El-Sherbiny, M. H. Yacoub, "Hydrogel scaffolds for tissue engineering: Progress and challenges," Global Cardiology Science and Practice, p. 38, 2013.

[4] A. C. Daly, L. Riley, T. Segura, J. A. Burdick, "Hydrogel microparticles for biomedical applications," Nature Reviews Materials, vol. 5, no. 1, pp. 20-43, 2020.

[5] C. A. Dreiss, "Hydrogel design strategies for drug delivery," Current Opinion in Colloid & Interface Science, vol. 48, pp. 1-17, 2020.

[6] X. Qi, L. Wu, T. Su, J. Zhang, W. Dong, "Polysaccharide-based cationic hydrogels for dye adsorption," Colloids and Surfaces B: Biointerfaces, vol. 170, pp. 364-372, 2018.

[7] C. D. Spicer, "Hydrogel scaffolds for tissue engineering: the importance of polymer choice," Polymer Chemistry, vol. 11, no. 2, pp. 184-219, 2020.

[8] V. Van Tran, D. Park, Y. C. Lee, "Hydrogel applications for adsorption of contaminants in water and wastewater treatment," Environmental Science and Pollution Research, vol. 25, no. 25, pp. 24569-24599, 2018.

[9] W. Jiao, W. Chen, Y Mei, Y. Yun, B. Wang, Q. Zhong, H. Chen, W. Chen "Effects of Molecular Weight and Guluronic Acid/Mannuronic Acid Ratio on the Rheological Behavior and Stabilizing Property of Sodium Alginate," Molecules, vol. 24, no. 23, 2019.

[10] F. Abasalizadeh, S. V. Moghaddam, E. Alizadeh, E. Akbari, E. Kashani, S. M. B. Fazljou, M. Torbati, A. Akbarzadeh, "Alginate-based hydrogels as drug delivery vehicles in cancer treatment and their applications in wound dressing and 3D bioprinting," Journal of biological engineering, vol. 14, no. 8, pp. 1-22, 2020.

[11] P. Jaipan, A. Nguyen, R. J. Narayan, "Gelatin-based hydrogels for biomedical applications," MRS Communications, vol. 7, no. 3, pp. 416-426, 2017.

[12] S. Afewerki, A. Sheikhi, S. Kannan, S. Ahadian, A. Khademhosseini, "Gelatin-polysaccharide composite scaffolds for 3D cell culture and tissue engineering: Towards natural therapeutics," Bioengineering and Translational Medicine, vol. 4, no. 1, pp. 96-115, 2018.

[13] D. Chawla, T. Kaur, A. Joshi, N. Singh, “3D bioprinted alginate-gelatin based scaffolds for soft tissue

engineering," International Journal of Biological Macromolecules, vol. 144, pp. 560-567, 2019.

[14] T. Pan, W. Song, X. Cao, Y. Wang, "3D bioplotting of gelatin/alginate scaffolds for tissue engineering: influence of crosslinking degree and pore architecture on physicochemical properties," Journal of Materials Science & Technology, vol. 32, no. 9, pp. 889-900, 2016.

[15] L. Baldino, S. Cardea, E. J. C. E. T. Reverchon, "Natural aerogels production by supercritical gel drying," Chemical Engineering Transactions, vol. 43, pp. 739-744, 2015.

[16] R. Rodríguez-Dorado, C. López-Iglesias, C. A. García-González, G. Auriemma, R. P. Aquino, P. Del Gaudio, "Design of aerogels, cryogels and xerogels of alginate: Effect of molecular weight, gelation conditions and drying method on particles' micromeritics," Molecules, vol. 24, no. 6, p. 1049, 2019.

[17] L. Baruch, M. Machluf, "Alginate–chitosan complex coacervation for cell encapsulation: Effect on mechanical properties and on long-term viability," Biopolymers: Original research on biomolecules, vol. 82, no. 6, pp. 570-579, 2006.

[18] Biological evaluation of medical devices, 10993-5, ISO, 2009.

[19] W. Y. Leong, C. F. Soon, S. C. Wong, K. S. Tee, S. C. Cheong, S. H. Gan, M. Youseffi, "In vitro growth of human keratinocytes and oral cancer cells into microtissues: an aerosol-based microencapsulation technique," Bioengineering, vol. 4.2, no. 43, pp. 1-14, 2017.

[20] C. S. Bento, S. Alarico, N. Empadinhas, H. C. de Sousa, M. E. Braga, "Sequential scCO2 Drying and Sterilisation of Alginate-Gelatine Aerogels for Biomedical Applications," The Journal of Supercritical Fluids, p. 105570, 2022.

[21] Q. Chen, X. Tian, J. Fan, H. Tong, Q. Ao, X. Wang, "An interpenetrating alginate/gelatin network for three-dimensional (3D) cell cultures and organ bioprinting," Molecules, vol. 25, no. 3, p. 756, 2020.

[22] C. M. Murphy, A. Matsiko, M. G. Haugh, J. P. Gleeson, F. J. O'Brien, "Mesenchymal stem cell fate is regulated by the composition and mechanical properties of collagen–glycosaminoglycan scaffolds," Journal of the mechanical behavior of biomedical materials, vol. 11, pp 53-62, 2012.

[23] A. M. Handorf, Y. Zhou, M. A. Halanski, W.-J. Li, "Tissue stiffness dictates development, homeostasis, and disease progression," Organogenesis, vol. 11, no. 1, pp. 1-15, 2015.

[24] J. Liu, H. Zheng, P. S. Poh, H.-G. Machens, A. F. Schilling, "Hydrogels for engineering of perfusable vascular networks," International journal of molecular sciences, vol. 16, no. 7, pp. 15997-16016, 2015.

[25] A. Barros, S. Quraishi, M. Martins, P. Gurikov, R. Subrahmanyam, I. Smirnova, A. R. C. Duarte, R. L. Reis, "Hybrid Alginate-Based Cryogels for Life Science Applications," Chemie Ingenieur Technik, vol. 88, no. 11, pp. 1770-1778, 2016.

[26] T. P. Nguyen, B. T. Lee, "Fabrication of oxidized alginate-gelatin-BCP hydrogels and evaluation of the

microstructure, material properties and biocompatibility for bone tissue regeneration," Journal of Biomaterials Applications, vol. 27, no. 3, pp. 311-21, 2012.

[27] L. Yuan, Y. Wu, J. Fang, X. Wei, Q. Gu, H. El-Hamshary, S. S. Al-Deyab, Y. Morsi, X. Mo, "Modified alginate and gelatin cross-linked hydrogels for soft tissue adhesive," Artificial cells, nanomedicine, and biotechnology, vol. 45, no. 1, pp. 76-83, 2017.

[28] F. Dehghani, N. Annabi, “Engineering porous scaffolds using gas-based techniques,” Current opinion in biotechnology, vol. 22, no. 5, pp. 661-666, 2011.

[29] W. Aljohani, L. Wenchao, M. Ullah, X. Zhang, G. Yang, "Application of sodium alginate hydrogel,", vol. 3, no. 3, pp. 19-31, 2017.